THE MINERALOGY AND GEOCHEMISTRY OF NEW COBAR Au-Cu MINERALIZATION IN THE REGOLITH AND EXPLORATION IMPLICATIONS FOR THE COBAR DISTRICT, WESTERN NSW.

K.M. Scott and K.G. McQueen

CRC LEME OPEN FILE REPORT 239

November 2008

CRCLEME

(CRC LEME Restricted Report 137R / E&M Report 728R, 2000
2nd Impression 2008)

THE MINERALOGY AND GEOCHEMISTRY OF NEW COBAR Au-Cu MINERALIZATION IN THE REGOLITH AND EXPLORATION IMPLICATIONS FOR THE COBAR DISTRICT, WESTERN NSW.

K.M. Scott and K.G. McQueen

CRC LEME OPEN FILE REPORT 239

November 2008

(CRC LEME Restricted Report 137R / E&M Report 728R, 2000
2nd Impression 2008)

Addresses and affiliations of Authors:

K.M. Scott
Cooperative Research Centre for Landscape Environments and Mineral Exploration
c/- CSIRO Exploration and Mining
P.O. Box 136
North Ryde
NSW 2113

K.G. McQueen
Cooperative Research Centre for Landscape Environments and Mineral Exploration
Faculty of Applied Science
University of Canberra
ACT 2601

TABLE OF CONTENTS

LIST OF FIGURES

LIST OF TABLES

LIST OF APPENDICES

SUMMARY

A study of mineralised and barren profiles at New Cobar has revealed the nature of dispersion of Au and its pathfinder elements within the top 30 m of the regolith. Gold mineralisation at the New Cobar deposit is associated with Ag, As, Bi, Cu, Mo, Pb, Sb, Se and W which are retained in the outcropping sub-vertical lode material. Sub-horizontal veins are also strongly mineralised for up to 6 m from the sub-vertical lodes with anomalous Au, Ag, Pb and Cu extending out for at least another 25 m. Thus, a lateral progression from Au-Ag-Pb-Cu to those elements, *plus* Bi, Mo, Se (and perhaps Sb and W), would be expected as mineralisation is approached.

In the mineralised profile, Au was separated from Ag during weathering to form pure supergene gold. Although there is no evidence of supergene enrichment of Au, there does appear to be surficial depletion of Au. Thus, use of the Au pathfinders in near-surface sampling during regional exploration is strongly recommended. The pathfinder elements are retained in Fe oxides with thousands of ppm Cu and Pb routinely observed in both hematite and goethite even in the near surface leached zone.

Weathering occurred in two main stages:- initially under acidic sulfate conditions to form alunite-jarosite minerals (hinsdalite) and Fe oxides and then under more arid conditions when Cl-rich overprinting occurs. However, because of the lack of mineralogical variation in the material so far studied, characterisation of material from 30 m to the base of oxidation is recommended when mining recommences.

1. Introduction

The Cobar Gold Field, near Cobar in western New South Wales, has produced over 2 million ounces of Au since the 1870's (Stegman, 2000) with a substantial proportion coming from oxidised ore. Despite this significant production, the characteristics of the Au ± Cu ores of the goldfield in the regolith are not well documented. However, recent open cut mining at the New Cobar mine(145° 52"E, 31° 28"S), 2 km south of Cobar township, has provided an opportunity to study the effects of weathering of Au-Cu mineralisation with depth.

The study reported here is the first part of a planned program to fully document the complete weathering profile at New Cobar. This report documents results from study of the upper 30 m of material from two profiles through the mineralised lode exposed in the southern wall of the pit and "barren material" about 25 m NW of that profile. The study also examines material from sub-horizontal veins adjacent to the main lode material and some samples from the northern end of the deposit. It specifically defines the behaviour of potential pathfinder elements including Ag, As, Bi, Sb, W and Zn as well as Au and Cu to better understand element movements during weathering and to make suggestions on how that knowledge may be used in on-going exploration in the Cobar region. These results may also help in seeking to understand the behaviour of oxide ore during metallurgical processing.

2. Geology

The New Cobar deposit occurs about midway along the 10 km long north-trending Cobar Gold Field (Figure 1). All the deposits in the goldfield are structurally controlled and located near the eastern margin of the early Devonian Cobar Basin (Glen, 1991). The New Cobar deposit occurs within siltstones and sandstones of the Great Cobar Slate, immediately west of a thrusted contact (Great Chesney Fault) with the more arenaceous Chesney Formation. The mineralisation occurs adjacent to a pronounced bend in the thrust. At its northern end, mineralisation is only 20 m from the thrust but is up to 150 m from the thrust at its southern end. Movement along the Great Chesney Fault was complex and probably occurred over an extended period (Stegman and Pocock, 1996).

Since the Late Cretaceous, rocks of the Cobar region have been subjected to chemical weathering under both wet-humid and, more recently, arid conditions. Relative tectonic stability for most of this period allowed the development of thick weathering profiles that underwent variable erosional stripping, particularly during the Late Miocene (Leah, 1996). Thus, preserved profiles vary considerably from thin (<3 m) profiles over weakly weathered near-surface saprock or bedrock to thick (up to 100 m) intensely weathered *in situ* profiles. The latter are characterised by a red silty loam soil. with surface ferruginous and lithic lag, overlying collapsed and ferruginised saprolite over bleached saprolite with variable ferruginous mottling above the water table. Older weathering profiles are commonly overprinted by the effects of later weathering under drier conditions marked by lower or fluctuating water table levels (Leah, 1996).

Silicification and ferruginisation associated with the mineralisation and its weathering at New Cobar has resulted in a positive surface expression of the deposit. The resulting hill has been subjected to erosional stripping for a long period and soils above the deposit were probably always thin. Aeolian material has probably been added to the soil during the Quaternary.

3. Mineralisation

Although Au was recognised as a component of the Cu ores at Cobar, Au was not sought as a commodity in its own right until the late 1880's when the association of silicification and Au was recognised at Fort Bourke Hill i.e. the New Cobar area (Stegman and Stegman, 1996). The Au mineralisation at New Cobar occurs in four steeply east-dipping Au-Cu lenses in the Great Cobar Slate adjacent to a thrusted contact with the Chesney Formation (see above). Paragenesis of the deposit is complex, with nine stages being recognised by Peak Gold Mines geologists (Leah and Roberts, 2000). Nevertheless it is clear that the economic mineralisation is present in the NW-trending sub-vertical quartz-breccia and base metal sulfide veins which occur within a broader envelope of disseminated pyrite. The Au occurs in three associations:– (i) most commonly as Ag-bearing Au with Bi minerals (along grain boundaries and as submicron inclusions), (ii) as generally Ag-poor, free Au along fractures and silicate grain boundaries and (iii) as Ag-rich Au associated with chalcopyrite (P.A. Leah, pers. comm., 1999).

Complete weathering at the deposit extends to about 60 m with partial oxidation extending another 40 m. The transition from primary ore to secondary mineralisation is marked by the appearance of supergene Cu minerals (native Cu and chalcocite) with Cu carbonates present where all of the sulfides, except pyrite, have oxidised. Weathering of the base metal sulfides has produced the Fe oxides and oxidate minerals of the alunite-jarosite group which dominate the profile to the surface. Gold is generally retained at similar levels to those in the primary ore up the profile, except in the top 10-15 m where it is strongly leached. There is no obvious zone of supergene Au enrichment (P.A. Leah, pers. comm., 2000).

In the southern portion of the open pit, several red-brown hematite-stained quartz breccia lodes are present within bleached saprolitic siltstones which are cut by brown goethitic sub-horizontal veins. The thickest lode (Southern Lode) is affected by structural contortions and varies in thickness from 4 m at the surface to 1 m thick at depth. Only a few centimetres of soil are present and, although the area has been disturbed by 19th century mining activity, soils there were probably never thick due to sustained erosion of the hill (Section 2).

4. Samples and Methods

A suite of 53 saprolitic samples from two profiles at the southern end of the pit (as at the end of the first phase of mining in late 1999) were collected with the assistance of Peak Gold Mines personnel during October 1999. Mineralisation at the southern end of the pit had lower grades than at the northern end but safety precautions precluded sampling through the higher grade material. Samples were collected at approximately 1 m intervals down the pit walls by abseilling. Sample locations were marked on the pit walls at the time of sampling and subsequently accurately measured by tape. The two profiles extended from the top of the pit down to a depth of 30 m (the safely accessible pit floor) and were from within the thickest quartz-rich lode in the southern wall (P1) and from barren material (P2), approximately 25 m to the NW (Figures 1 and 2). Because of flexure in the lode and access problems caused by ramps, the deepest mineralised samples (>25 m) were taken from nearly 20 m north of the higher mineralised samples and the background samples were only about 4 m from the lode (Figure 2). Vein and host-rock material was also collected from the sub-horizontal veins at

varying distances from the main lode at depths of 9.1 and 12.5 m (Figure 2). Brief sample descriptions are provided in Appendix 1.

After examination, 52 samples were crushed to <75 μm using a Mn-steel mill. They were then analysed by Analabs (Perth) for Al, Mg, Ca, Ti, Mn, P, S, Cu, Ni, Pb, Sr, V, Zn, and Zr by inductively coupled plasma emission spectrometry (ICP) and for Ag, Bi, Cd, Cu and Mo by inductively coupled plasma emission mass spectrometry (ICP-MS) after a HF/HCl/HNO$_3$/HClO$_4$ digestion. (It is recognised that possible incomplete dissolution of rutile and zircon means that the Ti and Zr values so obtained may represent minimum rather than "total" values for some samples.) Neutron activation analysis (NAA) for the "Au+31 suite" was also performed by Becquerel Laboratories (Lucas Heights) for each sample. Results are reported in Appendices 2-4.

After receipt of the chemical analyses, 18 samples were chosen as representative of specific depth intervals and were analysed mineralogically by X-ray diffraction, using graphite-crystal monochromated, Cu radiation.

The Fe oxides in 7 samples (including one from about 40 m depth toward the northern end of the pit; Appendix 5) were analysed by electron microprobe. Major elements were analysed using 20 second counting times but trace components (As, Bi, Cu, Pb, Se, W and Zn) were analysed using 100 second counting times to allow these elements to be determined down to a detection limit of 100 ppm.

5. Results

5.1 Mineralised and Barren Profiles

The analyses from the mineralised and barren profiles can be considered in four groups *viz.* upper 10 m, 10-15 m, 15-20 m, 26-30 m. Inspection of Table 1 indicates that the 15-20 m interval contains ore-grade material with As, Bi, Cu, Mo, Pb, Sb, Se and W associated with the Au. However, although Au is still quite high in deeper material, Au grades are at least an order of magnitude less in the material above 15 m. Despite such low Au contents in these upper intervals, the pathfinder elements are either much less depleted than Au (e.g. Cu, Mo, Se, W) or at similar levels, or even enriched relative to their abundances at 15-20 m (As, Bi, Pb, Sb).

Gold contents are consistently low (<70 ppb) in the barren profile and the pathfinder elements, with the exception of Pb, are also much lower than in the mineralised profile (cf. Tables 1 and 2). It should also be noted that Ag levels in the barren profile are higher than in the mineralised profile and, although lower, Cu and W are still quite anomalous in the barren profile. Relatively high values of Bi and Se in the 26-30 m interval in the barren profile probably reflect close proximity to the lode at this depth (Section 4; Figure 2).

Table 1. Average composition of intervals in the mineralised profile, New Cobar
(ppm, unless otherwise indicated)

Depth (m)	0-10	10-15	15-20	26-30
No. of Samples	10	6	4	4
Al (%)	1.55	1.36	0.96	1.13
Fe (%)	12.4	13.5	15.6	5.54
Mg	560	660	310	290
Ca	66	53	<50	<50
Na	180	390	150	<100
K (%)	0.31	0.47	0.20	0.28
Ti	1200	1700	730	380
Mn	59	63	69	44
P	92	140	88	130
S	450	580	630	200
Ag	1.1	1.0	1.5	2.1
As	150	92	44	52
Au (ppb)	94	130	2360	730 (410)
Ba	<100	<100	<100	<100
Bi	30	100	38	96
Cd	0.5	0.5	0.3	<0.1
Ce	28	25	20	18
Co	2	4	3	<1
Cr	31	47	29	22
Cs	1	2	<1	1
Cu	820 (620)	770	1300	520
La	13	13	7	5
Mo	9	14	27	8
Ni	<10	<10	<10	<10
Pb	600	960	990	540
Rb	26	34	22	<20
Sb	6	8	5	6
Sc	7	9	9	4
Se	13	39	81	39
Sr	7	6	5	3
Th	6	7	3	1
U	<2	<2	2	<2
V	29	36	19	12
W	9	13	52	29
Zn	66	54	49	53
Zr	48	49	26	14

Note: Values in parentheses represent averages obtained omitting an anomalously high value.

Table 2. Average composition of intervals in the barren profile, New Cobar
(ppm, unless otherwise indicated)

Depth (m)	0-10	10-15	15-20	26-30
No. of Samples	8	3	4	4
Al (%)	8.46	9.08	9.77	3.53
Fe (%)	3.24 (2.24)	4.29	4.30	3.28
Mg	4900	5100	5900	490
Ca	110	<50	73	150
Na	860	510	550	140
K (%)	3.80	3.90	4.33	0.36
Ti	3900	4000	4000	1600
Mn	160	62	65	38
P	550	130	160	130
S	520	260	480	500 (200)
Ag	1.8	1.9	1.3	1.1
As	3	10	6 (1)	57 (23)
Au (ppb)	31 (17)	24	67 (33)	61
Ba	770	780	970	100
Bi	1	1	3	20
Cd	<0.1	<0.1	<0.1	<0.1
Ce	68	52	47	32
Co	<1	2	1	1
Cr	100	130	130	37
Cs	9	11	13	1
Cu	210	140	160	370
La	40	28	26	13
Mo	1	1	2	1
Ni	12	20	12	46 (<10)
Pb	2100	710	750	700 (340)
Rb	270	290	330	22
Sb	3	2	3	3
Sc	18	20	20	7
Se	<5	<5	<5	6
Sr	18	12	20	5
Th	22	22	26	6
U	2	2	2	<2
V	110	94	120	22
W	10	8	10	14
Zn	33	20	20	45
Zr	100	110	110	43

Note: Values in parentheses represent averages obtained omitting an anomalously high value.

Relative to the mineralised profile, barren material shows higher Al, Mg, Ca, Na, K, Ti, P, Ba, Cr, REE, Rb, Sc, Sr, Th, U, V and Zr but lower Fe contents (Tables 1 and 2).

The mineralised profile shows strong development of Fe oxides, with goethite subsidiary to hematite. Muscovite and quartz persist through the profile but kaolinite is only strongly developed below 20 m (Figure 3). In the barren profile, quartz, hematite, muscovite and kaolinite persist through to the surface but goethite is not present except in 10 cm-thick Pb-rich low-angle veins in the top 5 m (Figure 4). Kaolinite is much more strongly developed than in the mineralised profile and hinsdalite (a Pb-Al-phosphate/sulfate member of the alunite-jarosite group) is commonly present. Both profiles show kaolinite relatively enriched relative to muscovite below 20 m. Iron oxides are also less abundant below 25 m, especially in the mineralised profile (Figures 3 and 4).

The Pb-rich low-angle veins in the top 5 m of the barren profile contain more abundant goethite than hematite and coronadite ± pyromorphite but are depleted in quartz, muscovite and kaolinite. Thus they are quite dissimilar to the surrounding material and are considered separately (see below).

5.2   Geochemistry and mineralogy of the sub-horizontal veins

Comparison of the geochemistry of the vein and host-rock material (Samples 138511A and B and 138513A and B; Appendix 3) indicates that there is no significant difference in their Au contents. However, when vein and adjacent host-rock material is considered relative to distance from the main sub-vertical lode, by 6 m away there is a marked decrease in Au, Bi, and Mo. Silver, As, Cu and W may also fall but Pb abundances are still high (Table 3).

Material from the sub-horizontal veins and immediate host rocks is mineralogically similar to material from the barren profile at a similar depth. All three sample types consist of abundant muscovite, kaolinite and quartz with Fe oxides (and possibly even some hinsdalite in the host rock). However, in contrast to other samples from both the mineralised and barren profiles, goethite is the dominant Fe oxide in sub-horizontal vein and host rock material.

The Pb-rich low-angle veins are also goethite-rich and contain hinsdalite + coronadite ± pyromorphite (Figure 4) but contain only low amounts of quartz, muscovite and kaolinite. These samples are extremely Pb-rich and also have high contents of Fe, Mn, P, S, Ag, As, Au, Cd, REE, Cu, Sb, Th, U, and Zn (Table 3).

5.3   Electron microprobe results

Trace and minor element contents of the Fe oxides are reported in Table 4. More Al, S, Cu, Se and Zn but less Pb and Bi are incorporated into goethite than into hematite from the same sample. Aluminium and Se are particularly abundant in goethite (and Bi in hematite) at around 15 m depth. Arsenic is more abundant in the Fe oxides at the top of the mineralised profile. Zinc and Pb are particularly abundant in the Fe oxides from the sub-horizontal veins and their immediate host rocks. Tungsten was only detected in the 40 m-deep sample where it occurs in both goethite and hematite with very high Bi and Cu and high abundances other chalcophile elements, except As and Zn. However up to 3100 ppm W was also found in rutile from the mineralised profile (Figure 5).

Table 3. **Average compositions of sub-horizontal veins and Pb-rich veins, New Cobar**
(ppm, unless otherwise indicated)

Distance from Lode (m)	Sub-horizontal veins		Pb-rich veins
	2-3	6-8	25
No. of Samples	5	2	2
Al (%)	6.34	5.12	4.80
Fe (%)	7.26	5.56	28.4
Mg	3300	(2900)	620
Ca	62	(250)	270
Na	750	320	190
K (%)	2.71	(2.14)	<0.2
Ti	3100	(2400)	380
Mn	690	88	1.63%
P	120	150	1.68%
S	250	190	1.03%
Ag	1.2	0.8	7.0
As	14	0.8	57
Au (ppb)	1260	5	4660
Ba	440	330	440
Bi	4	1	1
Cd	0.1	0.2	10
Ce	320	52	710
Co	5	4	180
Cr	120	65	86
Cs	10	8	<1
Cu	370	(250)	8300
La	16	(28)	470
Mo	5	1	1
Ni	10	15	27
Pb	1500	(1100)	12.7%
Rb	210	(180)	<20
Sb	2	1	9
Sc	18	10	44
Se	<5	<5	-
Sr	13	11	41
Th	18	12	29
U	3	2	39
V	110	62	150
W	8	5	-
Zn	180	(190)	930
Zr	92	62	20

Note: Values in parentheses represent averages obtained omitting an anomalously high value.

Table 4. Average trace element contents in hematite and goethite from profiles at New Cobar
(ppm, unless otherwise indicated) – determined by electron microprobe

Sample	Depth (m)	Fe oxide	No. of Analyses	Al$_2$O$_3$ (%)	P$_2$O$_5$ (%)	SO$_3$ (%)	As	Bi	Cu	Pb	Se	W	Zn
138491	3.6	Hem	6	0.78	0.09	0.43	540	<100	3200	1700	140	<100	470
		Goe	*4*	*0.99*	*0.09*	*0.68*	*500*	*<100*	*4200*	*840*	*110*	*<100*	*560*
138501	14.5	Hem	6	0.64	0.10	0.34	190	560	2300	2400	420	<100	110
		Goe	*6*	*2.49*	*0.09*	*0.70*	*120*	*240*	*6400*	*1600*	*740*	*<100*	*260*
138503	15.5	Hem	6	1.27	0.07	0.27	120	180	2200	1700	640	<100	310
		Goe	*6*	*3.07*	*0.10*	*0.31*	*190*	*<100*	*4000*	*750*	*1200*	*<100*	*480*
138504	16.8	Hem	6	0.79	-	-	<100	<100	920	2900	120	<100	500
		Goe	*5*	*2.20*	*-*	*-*	*140*	*<100*	*6500*	*200*	*180*	*<100*	*830*
138459	40	Hem	6	1.08	0.08	0.41	<100	730	7200	2700	570	300	140
		Goe	*6*	*1.88*	*0.07*	*0.94*	*<100*	*720*	*1.28%*	*1800*	*530*	*280*	*120*
138511A	9.1 (sub-horiz vein)	Hem	4	1.19	-	-	<100	<100	2000	2800	<100	<100	300
		Goe	*5*	*1.35*	*-*	*-*	*<100*	*<100*	*2000*	*4100*	*<100*	*<100*	*3400*
138511B	9.1 (host rock)	Hem	2	1.17	-	-	<100	<100	1400	3200	130	<100	1100
		Goe	*4*	*2.67*	*-*	*-*	*<100*	*<100*	*2400*	*3200*	*<100*	*<100*	*1500*

Table 5. Average trace element contents in colloform and residual hematite and goethite (sample 138503, 15.5 m depth, mineralised profile, New Cobar) (ppm, unless otherwise indicated) - determined by electron microprobe

	No. of Analyses	Al$_2$O$_3$ (%)	P$_2$O$_5$ (%)	SO$_3$ (%)	As	Bi	Cu	Pb	Se	W	Zn
Hematite Colloform	3	0.70	<0.05	0.31	<100	<100	1100	2400	100	<100	<100
Residual	3	1.69	0.11	0.24	210	370	3400	1000	1200	<100	520
Geothite Colloform	*3*	*2.25*	*0.11*	*0.28*	*230*	*120*	*3300*	*990*	*1200*	*<100*	*400*
Residual	*3*	*3.68*	*0.09*	*0.33*	*150*	*<100*	*4800*	*510*	*1200*	*<100*	*570*

In samples 138501, 138503 and 138504, both colloform and residual hematite and goethite are present (Figures 6 and 7). The colloform varieties are compositionally similar to the residual varieties, except in sample 138503 which has colloform varieties which are richer in Pb but lower in Al, Cu and Zn than the residual varieties (Table 5).

As well as occurring in substantial amounts in the barren profile (Figure 3), traces of hinsdalite were found during the electron microprobe study of samples 138491 and 138504 (i.e. at 3.6 and 16.8 m) in the mineralised profile.

High-fineness gold (i.e. with no detectable Ag) has been observed associated with Fe oxides in the quartz-rich portion of Au-rich samples at 15.5 m depth (Figure 8).

6. Discussion

6.1 Weathering of the New Cobar ore

Primary sulfide-rich mineralisation consists of assemblages of Au + pyrite + pyrrhotite + chalcopyrite + sphalerite + galena + Bi sulfides + magnetite (P.A. Leah, pers. comm., 1999). However, within 40 m of the surface, all the sulfides and magnetite are oxidised and their component elements (As, Bi, Cu, Pb, Se, W, Zn, as well as, S) are either dispersed or incorporated into Fe oxides ± hinsdalite in the weathered lode (Table 4). The bulk of the original gold was associated with Bi minerals and contained some Ag (Section 1) but the abundant Au in the weathered lode at 15-20 m is essentially Ag-free (Figure 8). Furthermore, above that depth, although Au contents are severely depleted, Ag is substantially retained (Table 1) i.e. Au and Ag behaved quite differently during weathering. The current arid conditions and Cl-rich groundwaters of the region would facilitate separation of Ag from Au during weathering (e.g. Mann, 1984; Webster and Mann, 1984). This depletion of Au relative to Ag in the top 15 m of the mineralised profile suggests that the leaching of Au, observed by Leah (pers. comm., 1999), is superimposed on original primary variations in Au in the deposit.

6.2 Sub-horizontal veins and Pb-rich veins

The sub-horizontal veins and their immediate host rock from within 15 m of the surface are mineralogically similar to sub-vertical lode material except that they contain goethite and hematite rather than only hematite (Figures 3 and 4). As indicated in Section 5.2, there is considerable migration of ore-associated elements into the immediate host rock such that there is little difference between the veins and host rock. Examination of such material at depth should be undertaken to establish whether this dispersion is primary or secondary. Nevertheless, the significant decrease in Au and its associated elements (except Pb and, perhaps, Ag and Cu) at distances greater than 6 m from the sub-vertical lode (Table 3) suggests that only the Pb (and Ag and Cu) contents of the sub-horizontal veins give a reliable indication of their proximity to ore in the regolith.

Lead-rich low-angle veins in the top 5 m of the barren profile also contain goethite as the dominant Fe oxide. These veins contain abundant hinsdalite and coronadite as well as pyromorphite. At Elura, the Cl-rich pyromorphite has replaced alunite-jarosite minerals at a late stage in the profile development (Scott, 2000). The development of pyromorphite in the New Cobar profile may similarly suggest the influence of late Cl-rich solutions. The low-angle veins are Au-rich with associated Ag, As, Cd, Cu, Pb, Th, U and Zn but low Bi and Mo contents (Table 3) i.e. an association quite different to the ore association seen in the weathered

lode. Thus, if the low-angle veins represent minor pods of New Cobar mineralisation, the retention of Cd, Th, U and Zn would suggest different weathering conditions to those affecting the main lode. Alternatively (and more likely), the low-angle veins represent Mo- and Bi-poor mineralisation quite different to that in the lode and it weathered in a local environment buffered by the presence of the enclosing silicates (i.e. under less acidic conditions than in the lode) so that the usually mobile Cd and Zn are retained.

6.3 Weathering of barren material

Barren material 25 m from the lode originally consisted of siltstone with disseminated pyrite. Within 40 m of the current surface the siltstone is weathered to assemblages of quartz, muscovite, kaolinite, hematite and hinsdalite. The substantial Pb, Ag and Cu contents of this barren material (Table 2) suggests that these elements were originally present as minor sulfides associated with the disseminated pyrite, the casts of which are retained to the surface (Appendix 1). Thus a Pb, Ag and Cu halo at least 25 m wide might be expected about similar Au-Cu lodes. The extent of such a halo and whether it extends to the east of the lode should be determined by further study prior to renewed mining at the deposit.

Samples from below 26 m are from close to the lode (~ 4 m away) and contain some of the ore-associated elements viz. As, Bi and perhaps Se and W. This suggests that significant dispersion occurred into the wall rocks either during the original mineralising event (as minor sulfides to form a primary dispersion halo) or during subsequent weathering. In either case, this suggests that an inner halo of As, Bi, Se and W may exist within the broader Au, Pb, Ag and Cu halo in the regolith.

6.4 Profile development

Chlorite is the dominant phyllosilicate alteration mineral in the New Cobar deposit (Stegman and Pocock, 1996). Such chlorite would readily weather to kaolinite but muscovite would tend to be much more resistant to weathering. Thus, the stronger development of kaolinite relative to muscovite below 20 m, in both mineralised and barren profiles, implies either original mineralogical variation or kaolinite-destructive weathering above 20 m. The former possibility could reflect a reduction in the amount of chlorite alteration as the intensity of alteration/mineralisation decreased in samples from above 20 m but the presence of good Au grades in the 15-20 m interval suggests that this is unlikely. Alternatively, destruction of kaolinite would free Al and Si, with Al being incorporated into Fe oxides (e.g. goethite at 15-17 m; Table 4) at relatively low pH (cf. Wollast, 1967) and freed Si leading to secondary silicification (as present in several samples above 12.5m in the mineralised profile: Appendix 1). Such silicification may reflect a late, arid overprint on original deep weathering at the New Cobar deposit (cf. Leah, 1996) with its vertical extent related to a former water table. However, the coincidence of the base of the low kaolinite abundance interval and the possible presence of secondary silicification in the part of the profile where Au contents are highest (in the 15-20 m interval) probably reflects original primary Au distribution rather than supergene enrichment of Au. Nevertheless, further study of the nature of the silicification in the profile should be undertaken.

Initial weathering at the New Cobar deposit would have been acidic and sulfate-rich as the sulfides oxidised. These conditions would have led to the formation of hinsdalite and the incorporation of S rather than P into the Fe oxides (cf. Scott, 1986). With the onset of aridity, Cl became an important component in the groundwaters. Chloride-rich solutions facilitated separation of Au from Ag (Mann, 1984; Webster and Mann, 1984) and also led to the replacement of acidic/sulfate-stable minerals by more Cl-rich varieties (e.g. pyromorphite). Similar Cl-overprinting is observed at Elura (Scott, 1994, 2000).

Regionally, secondary carbonates are also developed under the arid conditions but, at New Cobar, the continued local acidity, derived from on-going sulfate weathering at depth, appears to have restricted development of carbonate in the profile.

6.5   Implications for Exploration

The mineralised lode at New Cobar is characterised by the association of Au with Ag, As, Cu, Mo, Pb, Sb, Se and W and these elements are retained in the surficial lode material at the deposit even though the Au contents are only ~100 ppb i.e. Au is relatively low in the studied profile. The presence of low Au in lode material overlying economic grades at 15 m depth indicates that exploration for Au mineralisation in the Cobar region should use the pathfinder elements as well as Au in evaluating anomalies. This is especially so because, although Au at New Cobar appears to be subject to surficial depletion (P.A. Leah, pers. comm., 1999), the Fe oxides from the near surface samples still retain substantial pathfinder element contents (Table 4).

Surficial lode material tends to be hematitic and siliceous and as such would normally be routinely sampled during exploration. However, as indicated above, this material may not contain especially elevated Au contents. In this case, the trace element contents and paramagnetic characteristics of the quartz itself may be useful in establishing the genetic association with mineralisation (van Moort *et al.*, 1999).

A more commonly encountered exploration scenario might involve the sampling of ferruginous saprolite without quartz veins. Results from this study suggest that Au contents in such material may be ~30 ppb at 25 m from a mineralised lode. Such values are well above the regional background level for Au (<5 ppb) and hence are still quite anomalous. The presence of high Pb and accompanying Ag and Cu would confirm such Au contents as significant. As mineralisation is approached, anomalous Bi, Mo and Se (and perhaps Sb and W) might also be expected. However, because the Au (Figure 8) and its pathfinders (Table 4) appear to be associated with Fe oxides in the regolith, geochemical results may be highly susceptible to Fe variations in saprolitic samples. Thus ferruginous material should be preferentially sampled and geochemical results considered relative to Fe contents.

7.   Conclusions and Recommendations

Elevated abundances of Ag, As, Bi, Cu, Mo, Pb, Sb, Se and W occur with Au in the lode at New Cobar. These elements persist to the surface in readily detectible amounts and give confidence in interpreting relatively low Au contents as significant. Adjacent to the lode, the saprolite contains elevated Au, Ag, Pb and Cu. The presence of these pathfinders, especially Pb >700 ppm, at least 25 m from the lode indicates that a sizeable halo, that could be detected in multi-element regional exploration, exists. (The lateral extent of the Au and pathfinder anomaly in saprolite at New Cobar should be determined, prior to further mining.) The sub-horizontal veins are strongly mineralised within 6 m of the lode but do not appear to offer any advantage over saprolite sampling at distances further from the lode.

Weathering at the deposit appears to reflect two major events – acidic weathering to form sulfate- and base metal-rich Fe oxides and hinsdalite and a later Cl-rich weathering event under arid conditions when pyromorphite formed. This two-stage weathering history has implications for Au dispersion processes and hence the interpretation of regional geochemical surveys. Late-stage, secondary silicification may have affected the top 20 m of the profile at New Cobar – further evidence for this should also be sought because of silicification's potential effects on Au contents in surficial samples.

This study has focussed on detailed sampling from 30 m depth to the surface, that is, the depth typically sampled in regional exploration by surface and RAB drilling methods. However detailed study of samples from the supergene sulfide zone would be informative in providing a better framework for understanding of the elemental dispersion processes through the whole regolith profile. Study of deeper oxidised and supergene material would also provide information useful in understanding the processing behaviour of ore and the weathering characteristics of waste rock mined in the next phase of open pit development.

Other features which require further study are:–
(1) The extent of wall rock alteration/dispersion on both sides of the lode. This could be determined by rock (and possibly, soil) sampling. Sampling along a line along the southern edge of the pit prior to renewed mining is strongly recommended.
(2) The distribution of the Pb-rich low-angle veins and casts after pyrite in the "barren" saprolite (both vertically and laterally). This could be established by inspection and sampling of the pit walls.
(3) Trace element contents in the Fe oxides (colloform and residual) and other mineral phases to better relate elemental concentrations to events during weathering.

8. Acknowledgements

9. References

Cook, WG., Pocock, J.A. and Stegman, C.L.1998. Peak gold-copper-lead-zinc-silver deposit, Cobar. *In* Geology of Australian and Papua New Guinean Mineral Deposits (Eds: D.A. Berkman and D.H. Mackenzie), Australasian Institute of Mining and Metallurgy, Melbourne. pp.609- 614.

Glen, R.A., 1991. Inverted transtensional basin setting for Gold and Base metal deposits at Cobar, New South Wales. BMR Journal of Geology and Geophysics, 120: 13-24.

Leah, P.A., 1996. Relict Lateritic Weathering Profiles in the Cobar District, NSW. *In* The Cobar Mineral Field - A 1996 Perspective (Eds: W.G. Cook *et al*.), Australasian Institute of Mining and Metallurgy, Melbourne. pp.157-177.

Leah, P.A. and Roberts, C.A., 2000. New Cobar pit. *In* Central West Symposium Cobar 2000, Cobar field trip guide(Ed: M.J. Spry) CRC LEME, Perth. pp.8-12.

Mann, A.W., 1984. Mobility of gold and silver in lateritic weathering profiles: some observations from Western Australia. Economic Geology, 79: 38-49.

Scott, K.M., 1986. Elemental partitioning into Mn- and Fe-oxides derived from dolomitic shale-hosted Pb-Zn deposits, Northwest Queensland, Australia. Chemical Geology, 57: 395-414.

Scott, K.M., 1994. Lead oxychlorides at Elura, western NSW, Australia. Mineralogical magazine, 58: 336-338.

Scott, K.M., 2000. Elemental mobilities during the weathering of the Elura Zn-Pb-Ag orebody – the influence of mineralogy. *In* Central West Symposium Cobar 2000, Extended Abstracts (Eds: K.G. McQueen and C.L. Stegman) CRC LEME, Perth. pp. 94-97.

Stegman, C.L., 2000. The New Occidental deposit: variation on a theme. *In* Central West Symposium Cobar 2000, Extended Abstracts (Eds: K.G. McQueen and C.L. Stegman) CRC LEME, Perth. pp. 107-112.

Stegman, C.L. and Pocock, J.A., 1996. The Cobar Goldfield – A Geological Perspective. *In* The Cobar Mineral Field - A 1996 Perspective (Eds: W.G. Cook *et al*.), Australasian Institute of Mining and Metallurgy, Melbourne. pp.229-264.

Stegman, C.L. and Stegman, T.M., 1996. The History of Mining in the Cobar Field. *In* The Cobar Mineral Field - A 1996 Perspective (Eds: W.G. Cook *et al*.), Australasian Institute of Mining and Metallurgy, Melbourne. pp.3-39.

Taylor, G.F., Wilmshurst, J.R., Togashi, Y. and Andrew, A.S., 1984. Geochemical and mineralogical haloes about the Elura Zn-Pb-Ag orebody, western New South Wales. Journal of Geochemical Exploration, 22: 265-290.

Wollast, R., 1967. Kinetics of the alteration of K-feldspar in buffered solutions at low temperatures. Geochimica et Cosmochimica Acta, 31: 635-648.

Webster, J.G. and Mann, A.W., 1984. The influence of climate, geomorphology and primary geology on the supergene migration of gold and silver. Journal of Geochemical Exploration, 22: 21-42.

Van Moort, J.C., Li, X., Pwa, A., Bailey, G.M., Russell, D.W. and Butt, C.R.M., 1999. The use of electron paramagnetic resonance spectra and geochemical analysis of acid insoluble residues for recognising primary alteration haloes of gold mineralisation in the regolith. *In* New Approaches to an Old Continent. Proceedings of Regolith '98. (Eds. G. Taylor and C. Pain), CRC LEME, Perth. pp. 67-76.

Appendix 1. Sample descriptions, New Cobar

Sample No.	Depth (m)	Description
		Profile 1 (Mineralised)
138487	0.1	Brown Fe stone with brecciated quartz
138488	1.4	Brown silic gossan cut by Fe veins, chalcedony on facture
138489	2.4	Yellow-brown gossan with brecciated quartz
138490	3.6	Purple-brown Fe stone with brecciated quartz
138491	3.6	Brown silicified and ferrugnised siltstone
138492	5.1	Brown siliceous gossan
138493	6.6	Yellow-brown silicified and brecciated siltstone
138494	8.0	Purple-black gossanous siltstone, brecciated chalcedony on fracture
138495	8.6	Yellow-brown silic siltstone with brecciated quartz
138496	9.5	Yellow-brown silic siltstone
138497	11.3	Yellow-brown silic siltstone cut by quartz veins
138498	12.5	Purple-brown ferruginous siltstone cut by quartz veins. Pale chalcedony coating
138499	13.3	Red-brown and yellow brecciated siltstone
138500	13.8	Purple-yellow-brown brecciated and silicified siltstone
138501	14.5	Red and yellow silicified siltstone cut by Fe veins
138502	15.2	Buff silicified siltstone cut by quartz veins, Fe veins
138503	15.5	Red-brown Fe stone with brecciated quartz fragments
138504	16.8	Red-brown Fe stained brecciated quartz cut by Fe veins
138505	17.8	Red-brown silicified siltstone with brecciated fragments
138506	19.3	Brown stained silicified siltstone cut by red-brown Fe veins
138507	26.4	Brown stained siltstone cut by Fe veinlets
138508	27.6	Yellow-brown stained brecciated quartz
138509	28.6	Red-brown and jarositic stained quartz
138510	29.9	Red-brown and yellow stained brecciated quartz
		Sub-horizontal Veins
138511	9.1	Yellow and red stained siltstone (B) about black ferruginous vein (A)
138512	12.5	Red-purple ferruginous and silic siltstone with kaol
138513	12.5	Yellow and red stained siltstone (B) about ferruginous/siliceous vein (A)
138514	12.5	Bown Fe stained silic vein in Fe stained siltstone
138515	12.5	Red Fe stained siltstone
		Profile 2 (Barren)
138516	0.2	Purple casts after py in pale grey siltstone
138517	1.0	Grey siltstone with purple casts after py
138518	2.6	Grey siltstone with some casts after py
138519	3.6	Brown-purple siliceous vein?
138520	4.6	Grey siltstone with some casts after py
138521	4.9	Brown gossan with Cu staining
138522	6.0	Grey siltstone with casts and Fe veining
138523	7.0	Purple and grey siltstone
138524	8.5	Red-purple staining on grey siltstone, some casts after py
138525	8.5	White and purple stained siltstone with casts after py
138526	9.6	Pale purple stained siltstone with Fe veins and some casts after py

138527	10.8	Purple and grey fractured siltstone with Fe veins
138528	13.0	Purple stained siltstone
138529	14.8	Grey siltstone with purple staining about casts after py
138530	15.6	Red and purple staining in grey siltstone
138531	17.4	Grey siltstone with purple staining and casts after py
138532	18.6	Red-purple and grey siltstone with some casts after py
138533	19.9	Grey siltstone with purple Fe staining, casts after py
138534	25.9	White siltstone (with some py casts) cut by Fe/quartz veins
138535	27.7	Purple and yellow silicified siltstone cut by quartz/Fe veins
138536	28.8	Purple and buff siltstone cut by quartz/Fe veins
138537	29.7	Purple and buff siltstone cut by quartz/Fe veins

Appendix 2. Composition of samples, mineralised profile, New Cobar
(ppm, unless otherwise indicated)

Sample	138487	138488	138489	138490	138491	138492	138493	138494
Depth (m)	0.1	1.4	2.4	3.6	3.6	5.1	6.6	8
Al	11800	34000	29000	15600	7580	21500	7990	5750
Fe (%)	14.80	18.60	8.65	13.80	24.80	9.53	10.80	8.22
Mg	470	795	1080	600	185	930	275	205
Ca	95	85	60	55	70	55	65	60
Na (%)	-0.010	0.022	0.031	0.011	0.011	0.046	0.016	0.012
K (%)	-0.20	0.36	0.63	0.29	-0.20	0.70	-0.20	-0.20
Ti	400	940	1530	650	1330	1180	1310	1730
Mn	77	94	56	65	49	61	45	46
P	82	105	94	88	110	82	100	80
S	475	570	295	565	990	290	380	220
Ag	1.2	1.8	0.6	1.1	2.2	0.6	0.7	0.8
As	157.00	213.00	201.00	132.00	309.00	124.00	245.00	55.00
Au (ppb)	38.2	53.9	95.9	344.0	152.0	46.1	77.7	44.9
Ba	-100.0	389.0	-100.0	-100.0	-100.0	-100.0	-100.0	-100.0
Bi	10.6	18.1	33.6	23.7	50.6	27.7	71.6	27.8
Br	1.13	2.55	3.00	2.03	2.74	1.92	1.87	-1.00
Cd	0.3	0.9	0.3	0.6	1.4	0.2	0.8	0.3
Ce	11.70	32.30	30.60	17.80	31.20	27.40	35.60	32.40
Co	-1.00	2.34	1.95	1.08	1.57	1.01	3.10	1.97
Cr	39.4	31.7	41.4	31.1	53.2	28.9	20.5	15.0
Cs	-1.00	1.56	1.70	1.15	1.08	2.03	1.29	1.01
Cu	291	934	375	851	2630	525	786	414
Eu	-0.50	0.58	0.51	-0.50	0.86	0.54	0.82	0.65
Hf	-0.50	2.79	2.77	1.64	1.15	1.94	1.64	2.04
Ir (ppb)	-20.0	-20.0	-20.0	-20.0	-20.0	-20.0	-20.0	-20.0
La	5.66	9.05	14.10	8.63	10.20	12.70	16.40	15.60
Lu	-0.20	-0.20	-0.20	-0.20	-0.20	0.20	0.22	-0.20
Mo	2	5.1	8.4	6.8	15.3	8.2	16.8	10.9
Ni	-10	-10	-10	-10	-10	-10	-10	-10
Pb	736	967	467	578	803	594	520	518
Rb	-20.0	46.8	39.8	27.5	-20.0	56.2	-20.0	-20.0
Sb	1.98	4.67	4.06	3.21	8.45	4.34	16.70	8.16
Sc	5.77	11.30	9.76	6.24	8.50	7.71	5.87	4.16
Se	19.4	9.4	12.0	17.9	32.9	12.0	12.1	7.5
Sm	1.62	2.28	1.82	1.52	3.25	2.07	2.99	2.84
Sr	4	10	8	5	4	8	9	10
Ta	-1.00	-1.00	-1.00	-1.00	-1.00	-1.00	-1.00	-1.00
Te	-5.0	-5.0	-5.0	-5.0	-5.0	-5.0	-5.0	-5.0
Th	2.38	7.00	9.35	6.30	5.29	5.16	7.24	6.36
U	-2.00	-2.00	-2.00	-2.00	-2.00	-2.00	-2.00	-2.00
V	40	32	37	29	48	31	20	12
W	6.02	8.22	8.88	5.62	14.90	8.88	9.50	8.74
Yb	0.55	1.18	1.21	0.74	1.14	1.32	1.57	1.19
Zn	58	90	33	85	163	40	68	36
Zr	21	70	82	45	40	56	39	47

Sample	138495	138496	138497	138498	138499	1385	138501	138502
Depth (m)	8.6	9.5	11.3	12.5	13.3	13.8	14.5	15.2
Al	4790	17300	5890	4140	14000	22000	18700	17100
Fe (%)	10.10	5.02	10.10	20.40	10.40	17.70	16.10	6.10
Mg	155	835	195	135	560	1390	1090	575
Ca	55	60	65	75	75	55	-50	-50
Na (%)	-0.010	0.016	0.013	0.044	0.083	0.024	0.031	0.041
K (%)	-0.20	0.57	-0.20	-0.20	0.27	0.91	0.79	0.63
Ti	1290	1210	1950	1790	1780	1340	955	2110
Mn	32	62	53	44	65	82	93	41
P	98	72	205	175	135	125	90	80
S	565	135	450	1150	535	580	515	195
Ag	0.7	0.9	0.9	0.8	0.9	1	1.5	0.7
As	25.80	32.80	163.00	112.00	79.20	95.00	69.00	39.60
Au (ppb)	30.6	65.9	25.1	12.4	179.0	436.0	66.8	37.8
Ba	-100.0	-100.0	-100.0	-100.0	-100.0	-100.0	199.0	-100.0
Bi	26.2	11.1	110	59.2	40.5	134.5	197.5	76.3
Br	1.17	-1.00	1.78	3.47	4.99	1.66	1.14	1.01
Cd	0.5	-0.1	0.4	1.1	0.4	0.4	0.3	0.2
Ce	28.30	28.50	31.00	23.50	38.70	18.40	17.70	18.70
Co	4.61	1.37	3.15	7.39	5.25	4.03	2.89	2.13
Cr	26.5	20.3	33.6	73.7	36.3	64.0	49.7	25.5
Cs	-1.00	1.86	-1.00	-1.00	1.98	3.49	2.45	2.27
Cu	1145	304	621	1805	688	684	620	214
Eu	1.09	-0.50	1.04	1.39	1.49	0.86	0.82	0.53
Hf	1.46	1.80	2.25	1.59	2.27	1.90	1.31	2.20
Ir (ppb)	-20.0	-20.0	-20.0	-20.0	-20.0	-20.0	-20.0	-20.0
La	19.40	14.50	23.30	14.20	18.20	7.55	5.95	9.89
Lu	0.23	-0.20	0.23	0.29	0.28	0.28	0.22	-0.20
Mo	8.4	6.3	20.1	9.2	14.6	9.3	23	8.8
Ni	-10	-10	-10	-10	-10	-10	-10	-10
Pb	362	450	1155	1145	833	877	1115	638
Rb	-20.0	42.4	-20.0	-20.0	-20.0	54.6	72.8	47.6
Sb	2.93	5.79	19.20	4.87	7.57	5.64	4.89	5.17
Sc	7.85	5.87	6.49	10.80	9.26	13.80	8.60	6.35
Se	6.9	7.6	47.8	22.5	23.1	42.0	75.3	19.6
Sm	4.15	2.11	4.21	5.16	5.06	3.64	2.97	1.59
Sr	9	6	6	8	11	4	4	4
Ta	-1.00	-1.00	-1.00	-1.00	-1.00	-1.00	-1.00	-1.00
Te	-5.0	-5.0	-5.0	-5.0	-5.0	-5.0	-5.0	-5.0
Th	4.64	4.28	7.41	5.46	6.84	7.83	6.14	5.99
U	-2.00	-2.00	-2.00	2.17	-2.00	-2.00	-2.00	-2.00
V	19	20	23	52	29	47	39	26
W	6.45	13.80	11.70	8.33	11.30	18.90	14.40	12.90
Yb	1.44	0.99	1.54	1.97	1.91	1.84	1.45	1.19
Zn	59	30	45	97	52	51	45	33
Zr	35	41	52	46	54	51	35	56

Appendix 2 (cont.)

Sample	138503	138504	138505	138506	138507	138508	138509	138510
Depth (m)	15.5	16.8	17.8	19.3	26.4	27.6	28.6	29.9
Al	9120	11600	8980	8650	9580	16900	3380	15200
Fe (%)	16.30	19.70	10.70	15.80	5.91	7.03	3.05	6.16
Mg	180	445	265	320	125	585	100	345
Ca	-50	-50	-50	-50	-50	-50	-50	-50
Na (%)	-0.010	0.024	0.021	0.011	-0.010	0.011	-0.010	0.013
K (%)	-0.20	0.35	-0.20	0.23	-0.20	0.55	-0.20	0.35
Ti	355	590	1360	585	420	635	98	355
Mn	76	61	80	59	39	53	38	45
P	90	76	76	110	160	180	52	115
S	505	730	380	900	250	275	110	135
Ag	1.7	2.2	1.4	0.7	1.4	2	3.3	1.6
As	60.90	59.90	38.00	18.30	23.50	46.30	87.20	52.10
Au (ppb)	5970.0	241.0	1280.0	2000.0	1670.0	178.0	720.0	334.0
Ba	-100.0	-100.0	-100.0	-100.0	-100.0	-100.0	-100.0	-100.0
Bi	99.3	24.6	13.5	13.1	28	25.7	192	142
Br	1.27	3.05	2.15	-1.00	-1.00	1.15	-1.00	-1.00
Cd	0.3	0.5	0.2	0.2	-0.1	-0.1	-0.1	-0.1
Ce	16.40	21.40	35.90	20.70	16.70	32.10	5.75	14.60
Co	4.54	2.43	1.48	1.87	-1.00	1.05	1.46	-1.00
Cr	28.9	39.6	25.3	23.4	23.4	28.9	15.0	20.7
Cs	-1.00	1.43	-1.00	-1.00	-1.00	1.71	-1.00	1.27
Cu	968	880	1010	2280	675	587	237	550
Eu	-0.50	0.66	0.61	-0.50	-0.50	-0.50	-0.50	-0.50
Hf	0.56	1.36	1.70	0.92	0.72	0.88	-0.50	0.62
Ir (ppb)	-20.0	-20.0	-20.0	-20.0	-20.0	-20.0	-20.0	-20.0
La	8.04	5.27	5.13	9.33	2.83	11.60	2.65	1.99
Lu	-0.20	-0.20	0.20	-0.20	-0.20	-0.20	-0.20	-0.20
Mo	29.2	43.6	16.1	17.2	7.2	8.3	10.2	5.4
Ni	-10	-10	-10	-10	-10	-10	-10	-10
Pb	1080	1095	740	1020	345	670	637	500
Rb	-20.0	37.9	27.7	-20.0	-20.0	31.9	-20.0	24.9
Sb	6.51	5.28	4.14	4.74	2.89	4.17	16.10	1.91
Sc	7.95	10.00	8.16	10.80	4.17	5.64	1.04	4.48
Se	114.0	53.9	105.0	48.8	23.6	45.1	41.3	44.5
Sm	2.37	2.50	2.20	1.65	0.51	1.27	0.70	0.67
Sr	3	3	2	2	-1	2	-1	2
Ta	-1.00	-1.00	-1.00	-1.00	-1.00	-1.00	-1.00	-1.00
Te	-5.0	-5.0	-5.0	-5.0	-5.0	-5.0	-5.0	-5.0
Th	3.58	5.92	5.37	4.32	2.06	4.40	1.11	2.87
U	-2.00	-2.00	2.56	2.08	-2.00	-2.00	-2.00	-2.00
V	16	28	12	20	10	19	5	12
W	17.20	148.00	19.30	22.70	19.50	32.20	42.50	18.90
Yb	0.82	1.04	1.32	0.79	-0.50	0.65	-0.50	-0.50
Zn	60	49	46	42	33	23	138	46
Zr	14	24	42	23	13	25	-5	14

Appendix 3. Composition of samples, sub-horizontal veins, New Cobar
(ppm, unless otherwise indicated)

	138511A	138511B	138512	138513A	138513B	138514	138515
Dist(m) from profile	2	2	3	3	3	6	8
Al	50500	77500	35500	64000	89500	19900	82500
Fe (%)	13.30	12.70	10.60	11.70	1.31	2.50	8.62
Mg	2680	4390	770	3610	5170	965	4850
Ca	60	65	-50	65	95	-50	480
Na (%)	0.038	0.055	0.041	0.090	0.152	0.018	0.046
K (%)	2.25	3.69	0.51	2.80	4.28	0.68	3.60
Ti	2200	3620	1840	2950	4680	850	3880
Mn	2820	580	81	80	65	65	105
P	125	120	50	120	180	40	255
S	275	205	185	275	300	38	350
Ag	0.7	1	1.1	1.1	2.1	0.8	0.7
As	15.80	12.40	30.10	11.10	2.72	4.02	10.80
Au (ppb)	2380.0	2630.0	18.2	686.0	555.0	7.8	-5.0
Ba	369.0	542.0	-100.0	421.0	834.0	109.0	540.0
Bi	7.8	3.7	1.7	1.8	4.7	0.9	1.2
Br	1.83	1.56	1.04	3.56	3.94	-1.00	-1.00
Cd	0.2	0.1	0.1	0.1	-0.1	-0.1	0.3
Ce	1170.00	263.00	18.90	59.40	44.50	14.00	88.70
Co	9.87	6.28	2.81	3.79	1.11	1.20	7.39
Cr	103.0	171.0	102.0	136.0	107.0	31.8	97.4
Cs	7.31	12.50	2.76	9.91	14.70	2.42	13.10
Cu	516	409	480	397	40	79	429
Eu	1.66	1.79	0.71	1.21	0.69	-0.50	1.72
Hf	3.22	4.79	2.67	3.44	4.91	0.73	3.98
Ir (ppb)	-20.0	-20.0	-20.0	-20.0	-20.0	-20.0	-20.0
La	16.50	14.50	5.48	17.60	26.20	9.47	46.60
Lu	0.44	0.62	0.33	0.30	0.26	-0.20	0.75
Mo	5.7	6.1	2	2.9	2.6	1.1	1.4
Ni	-10	11	15	12	-10	-10	25
Pb	3310	1795	747	1180	519	282	1850
Rb	181.0	286.0	48.6	218.0	319.0	52.8	295.0
Sb	1.46	1.56	0.73	1.92	1.50	1.31	1.18
Sc	21.00	23.50	10.20	16.90	20.20	4.41	16.40
Se	-5.0	-5.0	-5.0	-5.0	-5.0	-5.0	-5.0
Sm	6.76	6.63	2.18	5.59	3.69	1.31	9.63
Sr	9	14	3	13	28	3	18
Ta	-1.00	1.35	-1.00	1.60	1.74	-1.00	1.62
Te	-5.0	-5.0	-5.0	-5.0	-5.0	-5.0	-5.0
Th	16.50	21.00	15.20	18.80	18.20	4.87	18.80
U	3.74	4.28	2.38	2.40	-2.00	-2.00	4.20
V	107	148	60	147	96	31	93
W	7.19	6.82	6.44	8.81	8.72	7.34	2.66
Yb	2.77	3.82	2.14	1.96	1.78	0.54	5.14
Zn	183	235	214	226	37	44	334
Zr	71	113	71	87	118	23	100

NOTE: A=vein, B=host-rock material

Appendix 4. Composition of samples, barren profile, New Cobar
(ppm, unless otherwise indicated)

	138516	138517	138518	138519	138520	138521	138522
Depth (m)	0.2	1	2.6	3.6	4.6	4.9	6
Al	87500	92000	90500	47000	94000	49000	85000
Fe (%)	1.28	3.53	1.10	33.50	0.70	23.30	3.00
Mg	5400	5380	5550	875	5440	350	4670
Ca	145	105	320	335	75	200	70
Na (%)	0.076	0.075	0.073	0.024	0.128	0.014	0.124
K (%)	4.25	4.17	4.07	-1.00	3.99	-0.50	3.70
Ti	4160	4060	4710	530	4510	220	3840
Mn	51	48	155	12600	310	19900	450
P	125	1120	135	6970	405	26500	1050
S	255	440	755	7170	565	13300	740
Ag	1	2.4	3.8	9	0.9	5.5	0.8
As	1.14	5.49	1.01	54.30	-1.00	59.60	1.73
Au (ppb)	-5.0	37.1	41.3	8120.0	32.3	1190.0	-5.0
Ba	1060.0	779.0	858.0	430.0	739.0	446.0	707.0
Bi	1.7	2.3	1.4	1	1.3	0.7	1.4
Br	-1.00	1.80	1.97	5.14	3.52	4.06	3.10
Cd	-0.1	-0.1	-0.1	6.5	-0.1	13.7	-0.1
Ce	60.10	114.00	71.20	971.00	67.90	436.00	53.50
Co	1.39	-1.00	-1.00	123.00	-1.00	229.00	-1.00
Cr	108.0	119.0	104.0	85.8	94.2	-20.0	104.0
Cs	10.60	11.00	10.50	-3.00	10.10	-2.00	9.67
Cu	88	146	143	8040	222	8630	352
Eu	1.10	1.08	1.65	3.56	1.11	7.59	1.04
Hf	4.55	4.60	5.14	-4.00	3.99	-1.00	4.12
Ir (ppb)	-20.0	-20.0	-20.0	-60.0	-20.0	-50.0	-20.0
La	32.00	54.10	37.10	590.00	36.60	335.00	32.10
Lu	0.38	0.48	0.39	0.80	0.39	0.60	0.41
Mo	3	2.1	1	1.2	2	1	0.6
Ni	11	-10	36	27	-10	27	12
Pb	351	4780	493	4.64	822	20.81	2080
Rb	285.0	304.0	290.0	-50.0	311.0	-40.0	256.0
Sb	1.52	3.62	1.43	5.61	0.98	10.60	1.59
Sc	18.70	20.30	19.90	48.50	17.90	38.00	16.80
Se	-5.0	-5.0	-5.0	-40.0	-5.0	-20.0	-5.0
Sm	4.76	7.14	5.80	19.10	5.51	21.50	4.03
Sr	23	28	20	62	21	20	14
Ta	-1.00	2.56	-1.00	-4.00	1.28	-2.00	1.36
Te	-5.0	-5.0	-5.0	-10.0	-5.0	-20.0	-5.0
Th	20.50	23.50	20.50	30.70	17.00	26.10	21.60
U	-2.00	3.57	2.18	18.40	2.26	59.70	-2.00
V	98	116	101	64	101	227	101
W	7.16	9.89	7.05	-5.00	3.72	-5.00	10.60
Yb	2.35	2.94	2.45	5.23	2.47	4.40	2.61
Zn	25	33	47	749	34	1070	49
Zr	109	111	119	31	111	8	98

Appendix 4 (cont.)

	138523	138524	138526	138527	138528	138529	138530
Depth (m)	7	8.5	9.6	10.8	13	14.8	15.6
Al	73000	68000	87000	64500	117000	91000	90500
Fe (%)	4.59	10.20	1.49	7.70	4.34	0.84	5.52
Mg	3870	3190	5730	4780	4360	6000	5060
Ca	60	55	-50	-50	50	-50	55
Na (%)	0.089	0.082	0.049	0.048	0.041	0.065	0.052
K (%)	3.50	2.67	4.08	3.41	3.12	5.16	4.36
Ti	3320	2560	4290	2750	4650	4640	3950
Mn	97	70	60	87	37	63	60
P	280	725	525	84	165	135	120
S	285	730	375	300	250	215	240
Ag	0.9	3.5	1.1	1.7	3.3	0.7	0.7
As	-1.00	2.57	13.30	17.40	12.50	-1.00	-1.00
Au (ppb)	-5.0	129.0	-5.0	61.7	-5.0	9.9	165.0
Ba	519.0	525.0	917.0	547.0	702.0	1100.0	874.0
Bi	1.2	1	0.8	0.9	1.1	0.9	1.1
Br	3.12	3.78	-1.00	-1.00	-1.00	1.41	-1.00
Cd	-0.1	0.2	-0.1	-0.1	-0.1	-0.1	-0.1
Ce	59.10	88.50	36.10	20.90	48.50	87.40	59.60
Co	-1.00	1.76	-1.00	-1.00	2.63	1.62	1.88
Cr	101.0	98.6	98.4	122.0	149.0	117.0	122.0
Cs	8.07	6.77	11.40	9.79	8.45	14.00	11.90
Cu	178	460	101	214	150	61	255
Eu	0.92	1.24	-0.50	0.69	1.06	1.34	1.18
Hf	3.75	3.28	3.99	3.28	5.47	4.79	4.55
Ir (ppb)	-20.0	-20.0	-20.0	-20.0	-20.0	-20.0	-20.0
La	33.60	65.90	26.90	10.10	25.80	47.70	31.90
Lu	0.28	0.26	0.33	0.32	0.46	0.43	0.38
Mo	0.6	0.4	0.3	1.5	0.7	0.1	-0.1
Ni	-10	-10	16	-10	41	13	18
Pb	1155	4650	2400	710	983	448	554
Rb	248.0	202.0	292.0	248.0	246.0	357.0	323.0
Sb	2.08	4.95	2.55	4.35	1.13	1.62	1.80
Sc	15.80	14.30	18.50	15.70	22.80	21.20	19.30
Se	-5.0	-5.0	-5.0	-5.0	-5.0	-5.0	-5.0
Sm	4.80	5.43	2.04	1.95	4.33	6.81	5.00
Sr	13	10	11	8	11	17	19
Ta	1.30	-1.00	1.21	1.49	2.07	3.02	-1.00
Te	-5.0	-5.0	-5.0	-5.0	-5.0	-5.0	-5.0
Th	22.80	27.50	18.30	19.40	23.70	22.90	27.20
U	-2.00	3.99	-2.00	-2.00	2.07	2.83	2.37
V	90	176	100	80	93	105	102
W	8.25	7.42	2.68	13.00	10.70	11.00	7.67
Yb	1.80	1.81	2.09	2.11	2.81	2.79	2.53
Zn	24	32	23	14	31	15	17
Zr	88	71	104	79	129	112	101

Appendix 4 (cont.)

	138531	138532	138533	138534	138535	138536	138537
Depth (m)	17.4	18.6	19.9	25.9	27.7	28.8	29.7
Al	92500	94000	113000	14300	32000	42500	52500
Fe (%)	0.95	7.07	3.66	1.45	2.31	5.65	3.71
Mg	5370	5610	6900	255	455	265	975
Ca	75	110	55	-50	-50	-50	510
Na (%)	0.061	0.049	0.056	-0.010	0.014	0.023	0.013
K (%)	4.22	4.17	4.56	-0.20	0.55	-0.20	0.67
Ti	4130	3770	4180	665	1290	1740	2590
Mn	67	68	65	36	33	43	40
P	125	235	135	-30	40	78	380
S	640	525	510	93	145	345	1370
Ag	0.7	0.7	2.9	1.3	1	1.4	0.8
As	-1.00	1.78	20.70	3.32	7.80	58.10	156.00
Au (ppb)	-5.0	-5.0	93.2	85.5	49.3	48.9	57.6
Ba	934.0	983.0	1140.0	-100.0	-100.0	106.0	187.0
Bi	1	3.2	5.1	2.4	30.9	29.3	18.8
Br	-1.00	-1.00	-1.00	-1.00	-1.00	1.37	-1.00
Cd	-0.1	-0.1	-0.1	-0.1	-0.1	-0.1	-0.1
Ce	39.90	38.30	50.30	12.10	24.00	42.20	48.40
Co	1.36	-1.00	1.70	-1.00	1.03	1.40	2.10
Cr	111.0	154.0	133.0	20.2	35.0	38.8	55.1
Cs	12.30	11.10	15.10	-1.00	2.38	-1.00	1.81
Cu	74	170	125	99	299	512	574
Eu	0.90	0.80	1.28	-0.50	-0.50	-0.50	0.58
Hf	4.67	4.31	5.33	0.64	1.65	2.08	3.06
Ir (ppb)	-20.0	-20.0	-20.0	-20.0	-20.0	-20.0	35.30
La	21.60	23.20	27.60	2.75	7.07	7.78	0.23
Lu	0.41	0.34	0.72	-0.20	-0.20	-0.20	1
Mo	3.2	2.5	1.3	0.8	1	1.4	170
Ni	10	-10	13	-10	-10	-10	1800
Pb	553	994	889	167	232	610	30.2
Rb	321.0	319.0	363.0	-20.0	37.5	-20.0	1.66
Sb	1.87	3.77	2.11	1.64	2.22	5.24	10.30
Sc	20.80	19.30	21.50	2.49	7.35	8.30	11.8
Se	-5.0	-5.0	-5.0	-5.0	-5.0	5.8	1.90
Sm	3.48	3.34	4.52	0.45	0.89	1.11	9
Sr	19	28	14	2	4	3	-1.00
Ta	2.34	-1.00	1.35	-1.00	-1.00	-1.00	-5.0
Te	-5.0	-5.0	-5.0	-5.0	-5.0	-5.0	9.00
Th	23.00	28.30	25.80	2.64	6.22	7.43	-2.00
U	-2.00	-2.00	3.79	-2.00	-2.00	-2.00	33
V	93	164	113	11	20	23	6.13
W	10.10	9.67	11.90	11.60	13.50	22.10	1.43
Yb	2.58	2.22	4.75	-0.50	0.85	1.11	48
Zn	19	24	18	12	28	91	71
Zr	102	103	127	16	36	47	

Appendix 5   Preliminary Sampling Results, New Cobar

Orientation Survey - New Cobar Pit   (August 1999)

Comparing saprolitic siltstone with the adjacent more ferruginous samples from 5 m depth on the eastern wall of the pit indicates that the ferruginous samples are enriched in the alkalis (Na, K, Ba, Cs and Rb), As, Au, (Ce) Co, Cr, Cu, (La), Pb, Sc, Th, W, Zn as well as Fe and Mn (Table A1). Significantly the ore-associated elements (As, Au, Cu, Pb, W and Zn) are enriched in the Fe-rich material. These elements plus Mo, Sb and Se are also enriched in the more highly mineralised samples from 10 m depth at the northern end of the pit (Table A1). Alkalis are low in the more highly mineralised samples.

Relative to regional values in weathered CSA Siltstone (Taylor *et al*., 1984) even the non-ferruginous saprolite is anomalous in Cu, Pb and perhaps, Au. Thus a significant geochemical halo exists about the deposit despite its strong structural control. The more-mineralised samples also tend to be hematitic rather than goethitic.

Consideration of individual samples indicates that Mn is high in 138414, with Pb high in 138415 and 138416 (X-ray Diffraction suggests that Pb probably occurs in alunite/jarosite type minerals and/or in the Fe oxides, as found at Wood Duck, McKinnons and Elura).

Gold and Ag occur in equal proportions in fresh mineralisation at The Peak ,with the amount of Ag :Au reaching 20:1 in near-surface workings (Cook *et al*., 1998) and in the Cu-rich samples from the northern end of the pit (Table A1). Thus the particularly high Au in 138416 (68 g/t) accompanied by low Ag (<5 g/t) probably indicates significant supergene enrichment of original gold relative to Ag. Such apparent variations in the behaviour of Ag during weathering may well reflect differences in the original mode of occurrence of the Ag and this should be investigated further by electron microprobe study.

It would also be worth investigating the mode of occurrence of Bi, Mo and W in samples from the highly mineralised northern end of the pit.

Table A1:Compositions of weathered material, New Cobar
(ppm, unless indicated otherwise)

Location	Regional*	Eastern End	Eastern End	Northern End	North End	
Depth(m)		Saprolite 5 m	Ferrug. 5 m	Mineralised 10 m	Cu- rich 40 m	
Fe%	1.82	1.56	18.6	18.9	12.8	
Ca	80	50	70	<50	-	
Na	-	<100	280	<100	<100	
K%	3.37	<0.20	1.82	<0.20	0.35	
Mn	160	36	470(88)	340(98)	50	
Ag	<5	<5	<5	<5	6	
As	10	10	18	480	30	
Au(ppb)	<5 **	18	55(7)	23000(970)	410	
Ba	780	<100	290	<100	120	
Bi	-	-	-	-	720	
Ce	-	20	60	1000(48)	18	
Co	<10	1	14(7)	9(5)	2	
Cr	-	22	66	52	18	
Cs	-	<1	7	<1	<1	
Cu	25	45	380	900	3200	
La	-	10	31	12	2	
Mo	-	<5	<5	14	12	
Pb	45	140	620(170)	810(440)	410	
Rb	-	<20	150	<20	34	
Sb	<5	2	2	12	6	
Sc	-	3	15	25(11)	11	
Se	-	<5	<5	110	120	
Th	-	5	12	8	2	
U	-	<2	2	3(<2)	2	
W	-	4	6	35	88	
Zn	7	31	460(300)	30	94	

*from Taylor *et al.* (1984) **Scott (1998, unpublished data)

Sample No.	Location/Depth	Description
138412	East wall / 5 m	Ferruginised siltstone
138413	East wall / 4 m	Black stained siltstone
138414	East wall / 6 m	Ferruginised veining in siltstone
138415	East wall / 5 m	Ferruginous veining in siltstone
138416	North wall / 10 m	Gossanous lode material
138417	North wall / 10 m	Gossanous lode material
138418	North wall / 10 m	Gossanous lode material
138459	North wall / 40 m	Gossanous lode material
138460	North wall / 40 m	Gossanous lode material

Sample	138412	138413	138414	138415	138416	138417	138418	138459	138460
Depth (m)	5	4	6	5	10	10	10	40	40
	East wall	East wall	East wall	East wall	North wall	North wall	North wall	North wall	North wall
Al	-	-	-	-	-	-	-	-	-
Fe (%)	10.10	1.56	23.20	22.60	29.00	13.30	14.30	14.50	11.00
Mg	-	-	-	-	-	-	-	-	-
Ca	100.0	50.0	50.0	50.0	50.0	-50.0	-50.0	-	-
Na (%)	0.031	-0.010	0.036	0.017	-0.010	-0.010	0.020	0.015	-0.010
K (%)	2.01	-0.20	2.52	0.93	-0.40	-0.20	-0.20	0.45	0.24
Ti	-	-	-	-	-	-	-	-	-
Mn	97.0	36.0	1230.0	79.0	824.0	79.0	117.0	54.80	44.50
P	-	-	-	-	-	-	-	-	-
S	-	-	-	-	-	-	-	-	-
Ag	-	-	-	-	-	-	-	8.80	3.40
As	8.36	10.20	22.60	23.20	775.00	386.00	282.00	32.20	27.10
Au (ppb)	12.0	17.8	-5.0	151.0	68000.0	1640.0	306.0	619.0	205.0
Ba	325.0	-100.0	391.0	143.0	-200.0	-100.0	-100.0	210.0	-100.0
Bi	-	-	-	-	-	-	-	875.00	557.00
Br	-1.00	1.21	2.03	1.50	3.15	1.05	1.86	-1.00	-1.00
Ce	60.80	20.30	77.70	40.70	3040.00	25.20	71.60	23.80	13.10
Co	3.86	1.47	28.40	9.36	15.80	3.10	7.48	1.79	1.28
Cr	65.3	21.8	86.2	46.6	87.1	32.4	37.6	22.6	13.5
Cs	5.98	-1.00	7.72	5.94	-1.00	-1.00	-1.00	-1.00	1.13
Cu	219.0	45.0	401.0	512.0	1780.0	462.0	466.0	3400.0	2900.0
Eu	1.75	-0.50	1.26	-0.50	1.86	-0.50	0.71	-0.50	-0.50
Hf	3.05	1.20	3.40	2.26	4.03	1.85	9.64	1.90	0.61
Ir (ppb)	-20.0	-20.0	-20.0	-20.0	-20.0	-20.0	-20.0	-20.0	-20.0
La	30.70	9.94	33.00	30.40	20.80	5.91	8.59	3.18	1.45
Lu	0.70	-0.20	0.39	0.25	0.59	-0.20	0.30	-0.20	-0.20
Mo	-5.0	-5.0	-10.0	-5.0	-10.0	25.8	11.8	9.6	14.6
Pb	39.0	140.0	305.0	1510.0	1540.0	419.0	466.0	543.00	267.00
Rb	161.0	-20.0	216.0	82.9	-20.0	-20.0	21.1	44.0	24.8
Sb	0.96	1.57	1.30	2.68	12.90	13.20	9.46	6.39	5.25
Sc	11.00	3.11	21.40	12.90	51.50	9.28	12.60	11.90	9.17
Se	-5.0	-5.0	-5.0	-5.0	49.4	150.0	131.0	131.0	109.0
Sm	9.16	1.87	7.12	1.46	9.51	2.09	2.83	1.75	1.21
Ta	-1.00	-1.00	-1.00	-1.00	-1.00	-1.00	1.07	-1.00	-1.00
Te	-5.0	-5.0	-5.0	-5.0	-5.0	-5.0	-5.0	-5.0	-5.0
Th	11.70	4.66	15.90	9.40	9.11	5.31	10.10	2.98	1.27
U	2.79	-2.00	6.30	-2.00	7.26	-2.00	-2.00	2.36	2.49
W	9.35	3.74	3.18	7.06	26.00	34.90	44.80	89.80	87.00
Yb	5.23	1.18	2.57	1.60	4.30	0.93	2.02	1.28	0.73
Zn	116.0	31.0	479.0	785.0	37.0	20.0	34.0	99.00	89.00
Zr	-500.0	-500.0	-500.0	-500.0	-500.0	-500.0	536.0	-500.0	-500.0
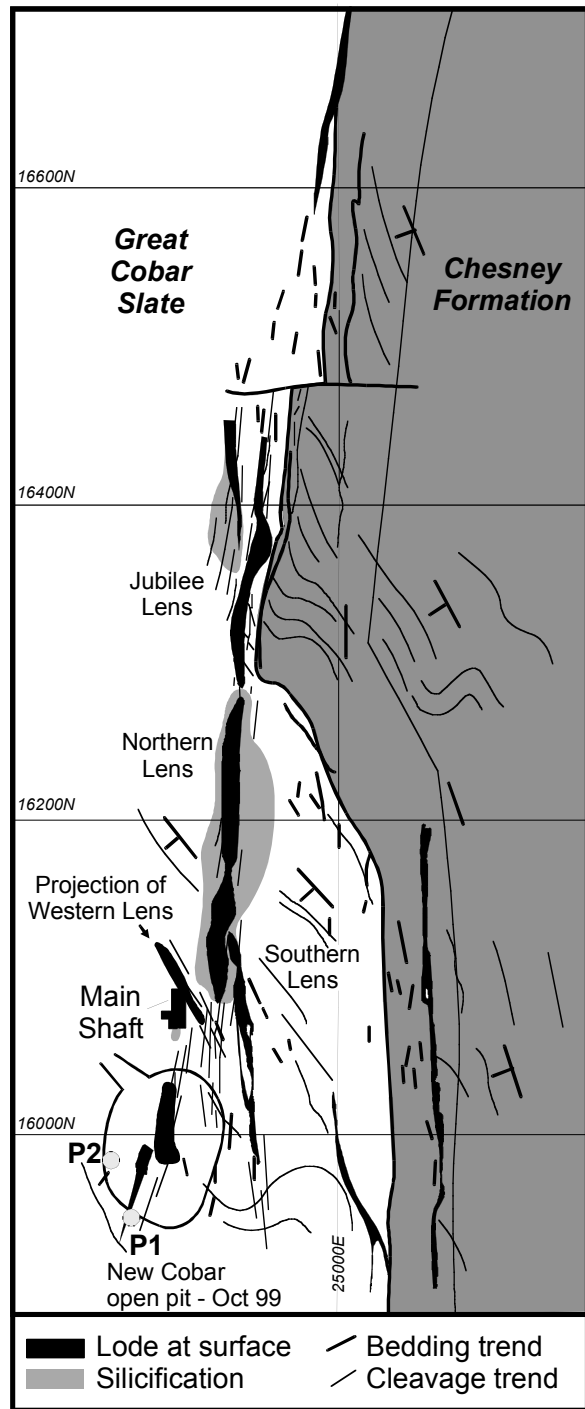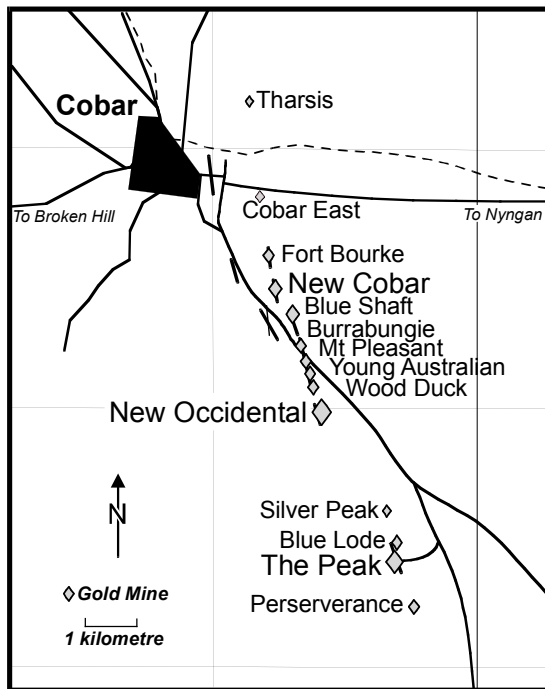
Figure 1.   The location of the New Cobar Deposit in the Cobar Gold Field (after Stegman and Pocock, 1996; Leah and Roberts, 2000)

Figure 2.   Location of samples from profiles, P1 and P2, south face, New Cobar Pit
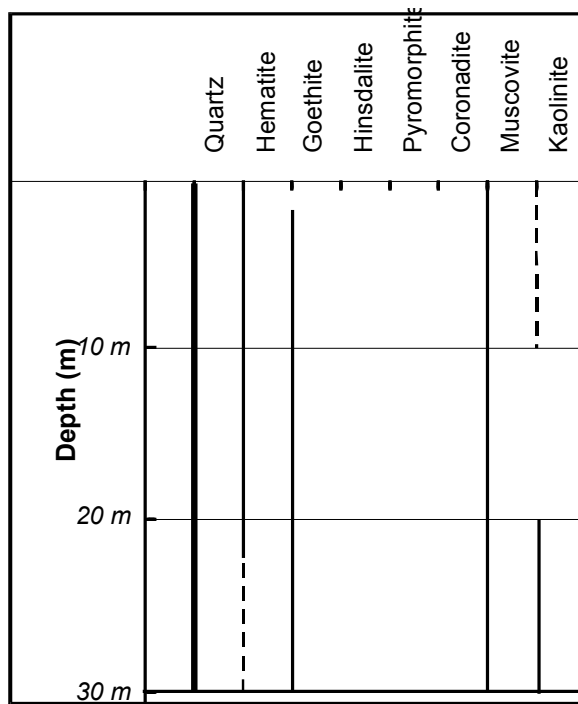
Figure 3.   Mineralogy of the mineralised profile, New Cobar (determined by XRD)
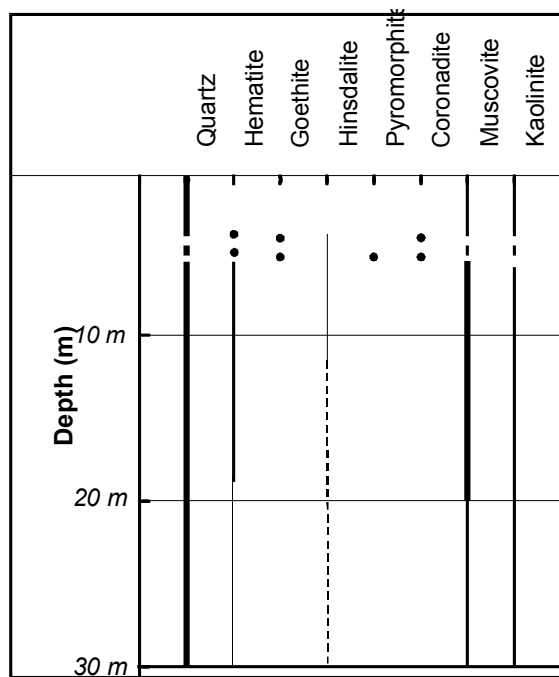
Figure 4.   Mineralogy of the barren profile, New Cobar (determined by XRD)
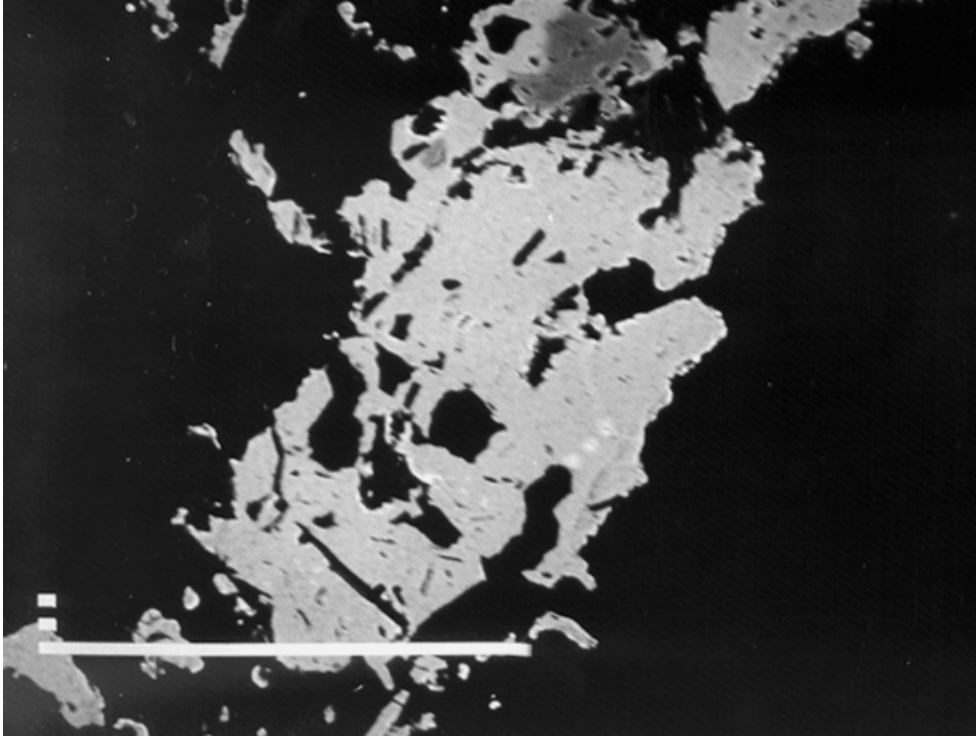
Figure 5.   W- bearing rutile (black inclusions), hinsdalite (pale grey) and goethite (dark grey) in hematite (grey). Sample 138491, Depth 3.6m. Scale bar = 100μm.
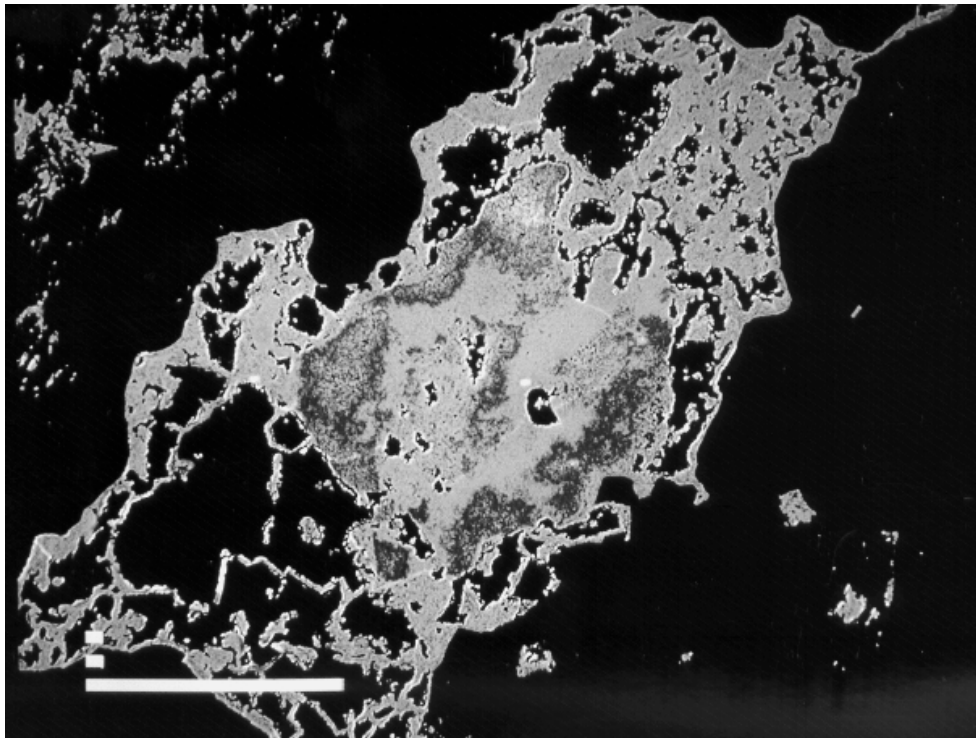
Figure 6.   Colloform hematite (grey) about residual hematite and goethite (dark grey). Sample 13850, Depth 14.5m   Scale bar = 100μm.
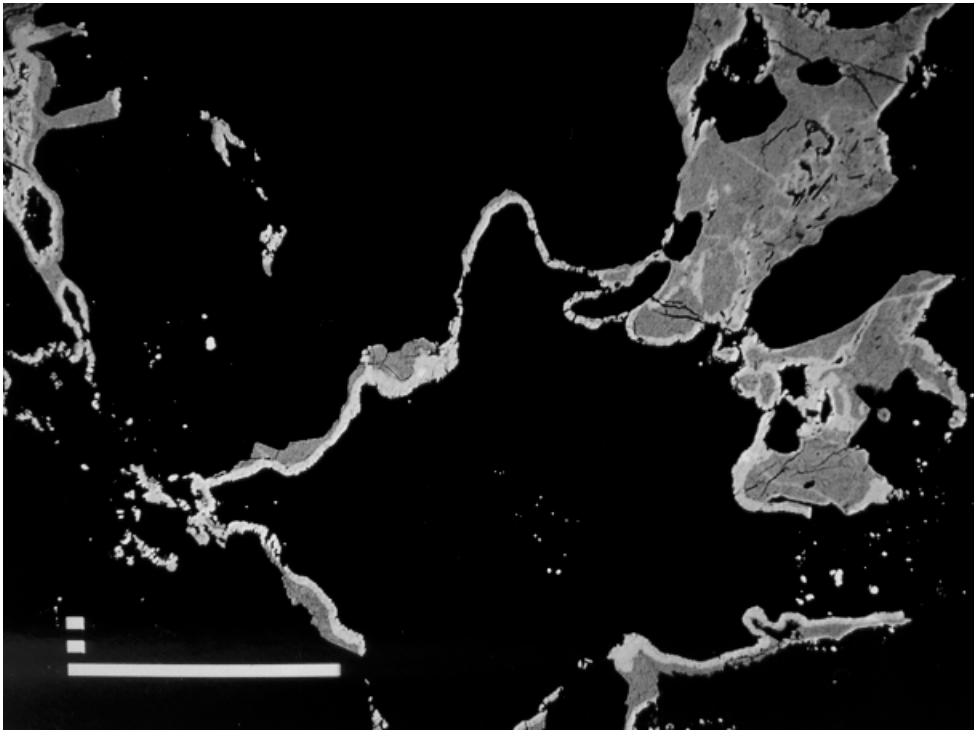
Figure 7.   Colloform hematite (grey-white) and goethite (grey) about void. Sample 138503   Depth 15.5m Scale bar = 100μm
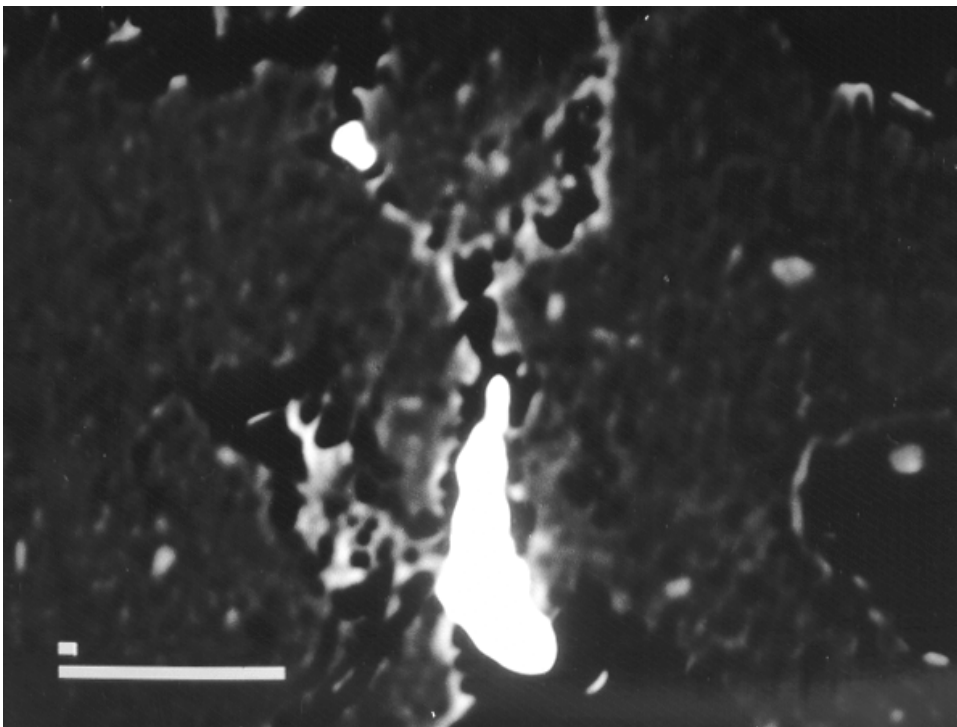
Figure 8.   Ag-free supergene gold (white) associated with goethite (dark grey, mottled). Sample 138503 Depth 15.5m Scale bar = 10μm